Bull Braz Math Soc, New Series 47(2), 545-559
© 2016, Sociedade Brasileira de Matemática
ISSN: 1678-7544 (Print) / 1678-7714 (Online)

Loss of hyperbolicity changes the number of wave groups in Riemann problems

Vitor Matos[1]*, Julio D. Silva[2] and Dan Marchesin[3]

Abstract. The main goal of our work is to show that there exists a class of 2×2 Riemann problems for which the solution comprises a single wave group for an open set of initial conditions. This wave group comprises a 1-rarefaction joined to a 2-rarefaction, not by an intermediate state, but by a doubly characteristic shock, 1-left and 2-right characteristic. In order to ensure that perturbations of initial conditions do not destroy the adjacency of the waves, local transversality between a composite curve foliation and a rarefaction curve foliation is necessary.

Keywords: hyperbolic conservation laws, Riemann problem, structural stability, transversality, adsorption systems.

Mathematical subject classification: 35L65, 35Q86, 35L67.

1 Introduction

The Riemann solutions for moderately nonlinear generic 2×2 systems of conservation laws are composed of a sequence of elementary waves, that is, contact discontinuities, rarefactions and shocks of various types, and of constant states. They are organized in waves groups, *i.e*, sequences of waves without any embedded constant state.

Received 28 March 2015.
*Corresponding author.
[1]Research supported by CNPq under grant PCI 170200/2014-0.
[2]The author thanks the Foundation CMG Industrial Research Chair Program.
[3]Research supported in part by CNPq under grants 402299/2012-4, 301564/2009-4 and 470635/2012-6, by FAPERJ under grants E-26/210.738/2014, E-26/201.210/2014, E-26/110.658/2012, E-26/111.369/2012, E-26/110.114/2013 and E-26/010.002762/2014, by ANP under grant PRH32-731948/2010, by Petrobras under grant PRH32-6000.0069459.11.4, as well as by CAPES under grant Nuffic-024/2011.

The following stands for generic Riemann initial conditions sets. Close to a strictly-hyperbolic and genuinely-nonlinear point, the Riemann solution is formed by two classical Lax waves, [6]. Failure of the two basic hypotheses of Lax, genuine non-linearity and strictly hyperbolicity, has effects that were studied over time. If genuine non-linearity is lost, the solution may be formed by wave groups with several waves rather than by two simple waves, [7]. In the presence of transitional (or undercompressive) waves (except for doubly characteristic transitional waves), there are three wave groups, [2, 13]. On the other hand, if doubly characteristic transitional waves were present in the solution then there would exist more than three wave groups. Transitional waves and high amplitude solutions for small amplitude data, [10], were found in systems where strictly hyperbolicity is lost.

The transport of a substance in a porous media without adsorption was studied in [3]. In that model, the flux function depends on the viscous ratio of the two fluids that changes with the concentration of the transported component. Despite this dependence, the family of problems is degenerate in the sense that some transversality condition fails everywhere.

In the present work, we study a class of conservation laws that models two-phase flow in porous media with adsorption of a transported component. These PDE's respect certain symmetries imposed by the physics. We show that there is an open set of initial conditions for which the Riemann solution consists of only one wave group. In this single wave group, a slow-rarefaction joins a fast-rarefaction through a doubly characteristic overcompressive shock. Within the class of problems we are concerned, this new kind of solution is structurally stable. The persistence of the doubly characteristic overcompressive shock is related to a transversality condition that depends on the adsorption term. We remark that this stability does not hold under general (and nonphysical) perturbations.

The new phenomenon of structurally stable Riemann solutions with a single wave group was found in [11], which built the complete Riemann solution for a system modeling thermal multiphase flow in porous media. However, the solution for a very similar Riemann problem in the context of polymer flooding was found in [4]. In [11] and here, structural stability is given in the sense of [1], *i.e.*, the wave groups that comprise the Riemann solutions persist if both L and R states are allowed to vary in open sets.

Due to the complexity of the original system, in [12] a new, simpler, family of systems with two conservation laws was coined to reproduce the wave patterns and interactions found in [11]. The effort was made of proving the existence of structurally stable Riemann solutions without intermediate constant state. However, since the physical nature of the original system was found, no additional effort was made to guarantee that the family of systems given in [12] itself represent any physical system.

The present work fills in the gap, showing that the phenomenon of structurally stable Riemann solutions without intermediate constant states does appear in a well known class of physical systems, namely the adsorption models, which is still simple enough to allow the proof of most of the facts found in [12]. Furthermore, we exploit properties of the adsorption models to provide a new and stronger proof of the transversality that supports the existence of the aforementioned phenomenon.

2 Transport model with adsorption

We consider a class of systems of two conservation laws that models the motion of two liquid phases in a porous media and the adsorption of a substance transported by a solvent. Here, $0 < s < 1$ represents the saturation of the solvent, and $0 \leq c \leq 1$ represents the concentration of the chemical component transported in the solvent. This is represented by the system of PDE's

$$\frac{\partial}{\partial t} G(s, c) + \frac{\partial}{\partial x} F(s, c) = 0, \tag{1}$$

where the accumulation and the flux functions are written as

$$G(s, c) = \Big(s\,,\ s\,c + \beta(c)\Big)^T, \quad F(s, c) = \Big(f(s, c)\,,\ c\,f(s, c)\Big)^T, \ \text{where} \quad f(s, c) = \frac{s^2}{\mathcal{D}(s, c)} \tag{2}$$

is the fractional flow function, with $\mathcal{D}(s, c) = s^2 + \mathcal{R}(c)(1-s)^2$. The viscosity ratio between liquid phases $\mathcal{R}(c)$ depends solely on the concentration. The adsorption term β is a smooth function of the concentration which satisfies the following inequalities:

$$\beta(c) > 0; \quad \dot{\beta}(c) > 0 \quad \text{and} \quad \ddot{\beta}(c) > 0; \tag{3}$$

in which each superimposed dot denotes a derivative with respect to the composition. In this work, the adsorption term β will play a similar role to the perturbation of the flux that appeared in [12]. Setting β to zero, System (1) reduces to the model studied by [3], [5] and [8]. Setting $\ddot{\beta} < 0$, System (1) reduces to the model studied by [4].

2.1 Eigenvalues, Rarefactions, Coincidence and Inflection locus

Rarefaction waves are smooth self-similar solutions of Eq. (1), which satisfy the generalized eigenvalue problem:

$$(DF - \lambda DG)\, r = \begin{bmatrix} f_{\mathrm{s}}(s,c) - \lambda & f_{\mathrm{c}}(s,c) \\ c f_{\mathrm{s}}(s,c) - c\lambda & f(s,c) + c f_{\mathrm{c}}(s,c) - (\dot{\beta}(c) + s)\lambda \end{bmatrix} r = 0. \quad (4)$$

By substituting $\lambda = f_{\mathrm{s}}(s,c)$ into Eq. (4), one easily obtains that its first column vanishes. Analogously, by substituting $\lambda = f(s,c)/(\dot{\beta}(c) + s)$ in Eq. (4), one easily verifies that the second line will equal c times the first one. Therefore, the eigenvalues of Eq. (4) are given as:

$$\begin{aligned} \lambda_s &= f_{\mathrm{s}}(s,c) = \frac{2\, s\mathcal{R}(c)(1-s)}{\mathcal{D}^2(s,c)} \quad \text{and} \\ \lambda_c &= \frac{f(s,c)}{s + \dot{\beta}(c)} = \frac{s^2}{\mathcal{D}(s,c)\,(\dot{\beta}(c) + s)}. \end{aligned} \quad (5)$$

Strict hyperbolicity is lost on the coincidence locus, defined as follows.

Definition 1. *The coincidence locus C is the null set of $\lambda_s - \lambda_c$.*

Here, C is the union of the vertical axis with a smooth curve. Indeed, from Eq. (5), we obtain that this curve is the zero level set of

$$\big(\mathcal{R}(c) + 1\big)s^3 + \mathcal{R}(c)\,\big(2\,\dot{\beta}(c) - 1\big)s - 2\,\mathcal{R}(c)\,\dot{\beta}(c). \quad (6)$$

A simple calculation verifies that (6) is smooth function with nonvanishing gradient.

Lemma 1. *The coincidence curve disconnects state space in two components (see Fig. 1b).*

Proof. To prove the lemma it is sufficient to observe that, for any $0 \le c \le 1$ fixed, the cubic polynomial $p_c(s) = \big(\mathcal{R}(c) + 1\big)s^3 + \mathcal{R}(c)\,\big(2\,\dot{\beta}(c) - 1\big)s - 2\,\mathcal{R}(c)\,\dot{\beta}(c)\big)$, see Eq. (6), has a single root $s \in [0,1]$. We have that $p_c(0) = -2\,\mathcal{R}(c)\,\dot{\beta}(c) < 0$ and $p_c(1) = 1$, therefore, the mean value theorem yields that $p_c(s)$ has at least one root in $[0,1]$. We now prove that this root is unique in $[0,1]$. The derivative $\dot{p}_c(s)$ is a parabola with positive leading coefficient, namely $\dot{p}_c(s) = 3(\mathcal{R}(c)+1)s^2 + \mathcal{R}(2\,\dot{\beta}(c) - 1)$, and $\dot{p}_c(0) = \mathcal{R}(c)\big(2\dot{\beta}(c) - 1\big)$. We have two cases: (i) for $\dot{\beta}(c) < 1/2$ we have $\dot{p}_c(0) < 0$, then the cubic p_c has a maximum for $s < 0$ and a minimum for $0 < s$. With no maximum in $0 < s < 1$, there can be only one root therein; (ii) for $\dot{\beta}(c) > 1/2$ the derivative $\dot{p}_c$ is positive for $s \in \mathbb{R}$, thus p_c has only one root. $\square$

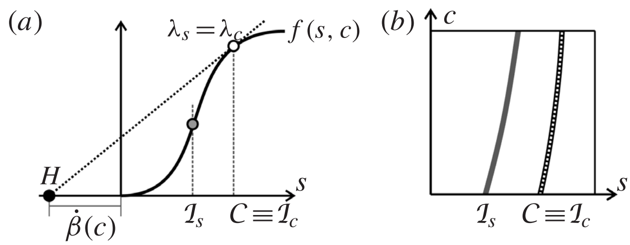

Figure 1: Relative position of inflections and coincidence locus. (a) Sketch of the fractional flow function $f(s,c)$. The eigenvalue λ_s is represented by the tangent to the graph of f. The eigenvalue λ_s is represented by the slope of the straight line that joins $H=(-\dot{\beta}(c),0)$ to $(s, f(s,c))$. Black dot: H. Gray dot: saturation inflection point. White dot: coincidence point. (b)Relative position on the space state of the saturation inflection, $\mathcal{I}_s$, and the coincidence locus, C. Gray curve: $\mathcal{I}_s$. Railway: C.

The eigendirections corresponding to λ_s and λ_c in Eq. (5) are spanned by:

$$r_s = (1,0)^T \quad \text{and} \quad r_c = \Big(f_{\mathrm{c}}(s,c)(\dot{\beta}(c)+s)\,,\ -f_{\mathrm{s}}(s,c)\big(\dot{\beta}(c)+s\big)+f(s,c)\Big)^T. \tag{7}$$

The matrix in (4) vanishes only at the intersection of the coincidence with the null set of $f_{\mathrm{c}}(s,c)$. We have $f_{\mathrm{c}}(s,c)=0 \Leftrightarrow \dot{\mathcal{R}}(c)=0$, therefore we chose the viscosity ratio to satisfy $\dot{\mathcal{R}}(c)\neq 0$ for all $0\leq c\leq 1$, thus impliying that the eigenvector of the compositional family r_c does not vanish in state space. We now focus on the states for which genuine nonlinearity is lost. The Inflection locus associated to the saturation family is

$$\begin{aligned}\mathcal{I}_s = \Big\{&(s,c)\mid \nabla\lambda_s(s,c)\cdot r_s(s,c) = 2\,\mathcal{R}(c)\\ &\times\Big(2\left(\mathcal{R}(c)+1\right)s^3 - 3\left(\mathcal{R}(c)+1\right)s^2+\mathcal{R}(c)\Big)=0\Big\}.\end{aligned} \tag{8}$$

Lemma 2. *The saturation inflection curve disconnects the state space in two components (see Fig. 1b).*

Proof. As was done in the previous Lemma we intend to show that, for any fixed $0\leq c\leq 1$, the cubic polynomial $q_c(s)=\nabla\lambda_s\cdot r_s(s,c)$ has a single root in $s\in[0,1]$. Notice that, since the leading coefficient of q_c is positive, we have from $q_c(0)=2\mathcal{R}(c)^2>0$ and $q_c(1)=-2\,\mathcal{R}(c)<0$ that its first root must be smaller than 0, because $\lim_{s\to-\infty} q_c(s)=-\infty$; its second root must lie in the interval [0, 1], because of the mean value theorem; and its third root must be greater than 1, because $\lim_{s\to\infty} q_c(s)=+\infty$. □

The Inflection locus associated to the compositional family is

$$\mathcal{I}_c = \Big\{(s,c) \mid \nabla\lambda_c(s,c)\cdot r_c(s,c) = \frac{\Big(f_s(s,c)\big(\dot\beta(c)+s\big) - f(s,c)\Big) f(s,c)}{\big(\dot\beta(c)+s\big)^2}\,\ddot\beta(c) = 0\Big\}, \tag{9}$$

Notice that the compositional inflection $\mathcal{I}_c$ and the coincidence C are the same curve, because $\ddot\beta(c) > 0$. One can verify through the use of geometrical arguments that $\mathcal{I}_s$ lies on the left-hand side of $\mathcal{I}_c \equiv C$, see Figure (1b). The concentration c decreases throughout a rarefaction of the compositional family, since $\nabla\lambda_c(s,c)\cdot r_c(s,c)$ equals the second coordinate of $r_c(s,c)$ multiplied by the factor $-f(s,c)\ddot\beta(c)/\big(\dot\beta(c)+s\big)^2$, which is negative. The rarefactions are depicted in Figure 2.

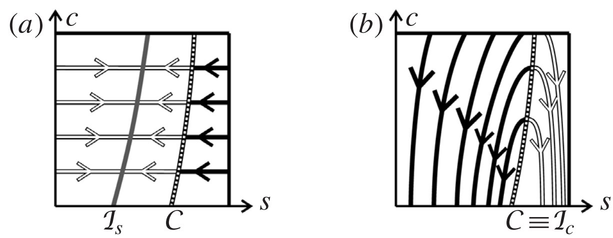

Figure 2: Railway: coincidence and inflection of compositional family. Solid line: slow rarefactions. Double line: fast rarefactions. Arrows point to increasing speed direction. (a) Rarefactions of saturation family. Gray line: inflection of saturation family. (b) Rarefactions of compositional family.

2.2 Hugoniot curve

Discontinuous solutions of Eq. (1) must satisfy the Rankine-Hugoniot relation:

$$F(s,c) - F(\grave{s},\grave{c}) - \sigma\big(G(s,c) - G(\grave{s},\grave{c})\big) = 0. \tag{10}$$

For a fixed $(\grave{s},\grave{c})$ in state space one is usually concerned with the locus of states (s,c) that satisfy Eq. (10); the resulting set is called the Hugoniot locus of the base state $(\grave{s},\grave{c})$. It satisfies:

$$\mathcal{X}\big(\beta(c) - \beta(\grave{c})\big) + \mathcal{Y}\,(c-\grave{c}) = 0, \quad \text{where} \tag{11a}$$

$$\mathcal{X}(s,c,\grave{s},\grave{c}) = s^2\,(1-\grave{s})^2\,\mathcal{R}(\grave{c}) - \grave{s}^2\,(1-s)^2\,\mathcal{R}(c), \quad \text{and} \tag{11b}$$

$$\mathcal{Y}(s,c,\grave{s},\grave{c}) = s^2\,\grave{s}\,(1-\grave{s})^2\mathcal{R}(\grave{c}) - s\,\grave{s}^2\,(1-s)^2\,\mathcal{R}(c) - s^2\,\grave{s}^2(s-\grave{s}). \tag{11c}$$

From (11a) we see that $c = \grave{c}$ belongs to the Rankine-Hugoniot curve.

The shock speed is given by:

$$\sigma(\grave{s}, \grave{c}, s, c) = \frac{s^2(1-\grave{s})^2\mathcal{R}(\grave{c}) - \grave{s}^2(1-s)^2\mathcal{R}(c)}{\mathcal{D}(s, c)\,\mathcal{D}(\grave{s}, \grave{c})}. \tag{12}$$

We outline the Hugoniot loci close to the coincidence in Figure 3. This figure is based on both analytic and numerical evidence; major computations were performed in Maple, [9].

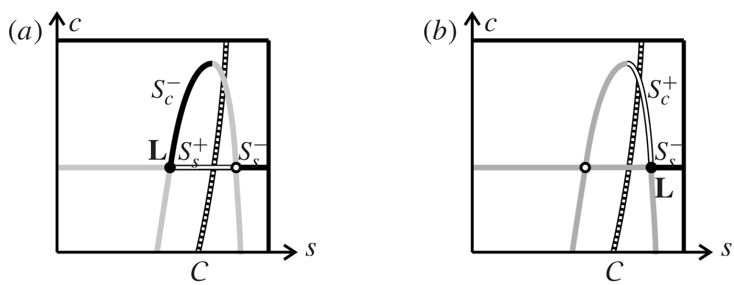

Figure 3: Black dot: left state **L**. Solid line: slow shocks. Double line: fast shocks. Gray lines: Hugoniot points that do not represent shocks. Railway: coincidence. (a) Hugoniot for **L** on left of the coincidence. Black dot: extension of **L** (doubly characteristic overcompressive shock). (b) Hugoniot for **L** on right of the coincidence.

2.3 Doubly characteristic shock

The construction of the Riemann solution relies on the fact that for any state $(\grave{s}, \grave{c})$ in a neighbourhood of the coincidence curve there is a companion $(\acute{s}, \acute{c}) \neq (\grave{s}, \grave{c})$ that lies on the intersection of the two branches of the Hugoniot locus, such that the shock between $(\grave{s}, \grave{c})$ and $(\acute{s}, \acute{c})$ is doubly characteristic with respect to the compositional speed: $\lambda_c(\grave{s}, \grave{c}) = \sigma = \lambda_c(\acute{s}, \acute{c})$, where σ is the shock speed in (10). Thus we introduce the following notation: for a set γ (typically, a curve) in state space, the extension set is

$$\mathcal{F}(\gamma) = \left\{ (\acute{s}, \acute{c}) \mid \exists (\grave{s}, \grave{c}) \in \gamma;\ \acute{c} = \grave{c} \text{ and } \sigma = \lambda_c(\grave{s}, \grave{c}) \right\}. \tag{13}$$

Here the extension is the map defined by associating to every state $(\grave{s}, \grave{c})$ near the coincidence curve its pair $\mathcal{F}(\grave{s}, \grave{c})$, for which one can construct a doubly characteristic shock. This can be proved in a similar fashion as was done in [12], if one assumes that the compositional branches of the Hugoniot locus are regular (here we just verified numerically this fact). The extension map can be rewritten as:

$$\mathcal{F}(\grave{s},\grave{c}) = \big(\acute{s}(\grave{s},\grave{c}),\grave{c}\big), \tag{14}$$

where $\acute{s}(\grave{s},\grave{c})$ is defined implicitly by $(\acute{s}-\grave{s})\,\mathcal{E}(\grave{s},\grave{c},\acute{s}) = 0$, and

$$\begin{aligned}\mathcal{E}(\grave{s},\grave{c},\acute{s}) &= \big(\mathcal{R}(\grave{c})+1\big)\,\grave{s}^2\,\acute{s}^2\\ &+\Big(\grave{s}\,\big(\dot{\beta}(\grave{c})-1\big)+\dot{\beta}(\grave{c})\,\big(\grave{s}-1\big)\Big)\,\mathcal{R}(\grave{c})\,\acute{s}+\grave{s}\,\dot{\beta}(\grave{c})\,\mathcal{R}(\grave{c}).\end{aligned} \tag{15}$$

Therefore, $\mathcal{E}(\grave{s},\grave{c},\acute{s}) = 0$ excludes from the extension the trivial solution $(\grave{s},\grave{c})$. We intend to show that the extension of compositional integral curves is transversal to the compositional eigen-direction field. First we need a definition:

Definition 2. *The Singular Extension locus is the set of* $(\grave{s},\grave{c})$ *where* $\mathcal{E}$ *has a double root* $\acute{s}$.

This set will be the non-trivial (*i.e.*, different from the coincidence curve) part of state space for which the extension of the compositional rarefactions will intersect tangentially the compositional eigen-direction field.

We record for later use the discriminant of $\mathcal{E}$ given in Eq. (15):

$$\begin{aligned}4\,\dot{\beta}(c)\,\big(\mathcal{R}(c)+1\big)\,s^3+\mathcal{R}(c)\,\big(2\,\dot{\beta}(c)-1\big)^2\,s^2\\ -2\,\mathcal{R}(c)\,\beta(c)\,\big(2\,\dot{\beta}(c)-1\big)s+\mathcal{R}(c)\,\dot{\beta}^2(c).\end{aligned} \tag{16}$$

Lemma 3. *Let us denote by* $\gamma(t)$, $\dot{\gamma}(t) = r_c(\gamma(t))$ *an integral curve of the composition family. Assume that no* $(\grave{s},\grave{c}) \in \gamma$ *is part of the Coincidence Locus or the Singular Extension Locus. Then the extension of* γ *is transversal to the composition eigen-direction field, defined in Eq.* (7). *(The extension may lie outside of the physical domain.)*

Proof. Any non-null vector in the tangent space of $\mathcal{F}(\gamma(t))$ is parallel to $\frac{d}{dt}\mathcal{F}(\gamma(t))$ which equals:

$$\begin{aligned}\frac{d}{dt}\mathcal{F}(\gamma(t)) &= \mathrm{D}\mathcal{F}(\gamma(t))\dot{\gamma}(t)\\ &= \begin{bmatrix} -\dfrac{\mathcal{E}_{\grave{s}}(\gamma(t))}{\mathcal{E}_{\acute{s}}(\gamma(t))} & -\dfrac{\mathcal{E}_{\grave{c}}(\gamma(t))}{\mathcal{E}_{\acute{s}}(\gamma(t))}, \\ 0 & 1 \end{bmatrix} r_c(\gamma(t)),\end{aligned} \tag{17}$$

where the derivatives on the first row were calculated by using the implicit function theorem in Eq. (15). Let us fix a t^*, and write $\gamma(t^*) = (\grave{s},\grave{c})$. For this choice of the parameter, there will correspond a doubly characteristic extension, which we will denote by $(\acute{s}, \acute{c})$. Using this notation, the condition of transversality between $\mathrm{D}\mathcal{F}(\grave{s}, \grave{c})r_c(\grave{s}, \grave{c})$, given by Eq. (17), and $r_c(\acute{s}, \acute{c})$ can be written as:

$$\mathcal{T}(\grave{s}, \grave{c}, \acute{s}) = \det\left[\, \mathrm{D}\mathcal{F}(\grave{s}, \grave{c})r_c(\grave{s}, \grave{c}),\ r_c(\acute{s}, \acute{c})\,\right] \neq 0. \tag{18}$$

The numerator of $\mathcal{T}$ is a fifth degree polynomial on $\acute{s}$. We obtained the resultant of $\mathcal{T}$ and $\mathcal{E}$ (as polynomials on $\acute{s}$ with coefficients on $(\grave{s}, \grave{c})$) with the Maple software [9]. The resultant is the product of the following seven factors:

$$\dot{\beta}(\grave{c}), \quad \ddot{\beta}(\grave{c}), \quad \mathcal{R}(\grave{c}), \quad \mathcal{R}(\grave{c})+1, \quad \mathcal{D}(\grave{s}, \grave{c}), \quad \grave{s} \tag{19a}$$

$$\Big(\big(\mathcal{R}(\grave{c})+1\big)\,\grave{s}^3 + \mathcal{R}(\grave{c})\,\big(2\,\dot{\beta}(\grave{c})-1\big)\,\grave{s} - 2\,\mathcal{R}(\grave{c})\,\dot{\beta}(\grave{c})\Big) \quad \text{and} \tag{19b}$$

$$\begin{aligned} &4\,\dot{\beta}(\grave{c})\,\big(\mathcal{R}(\grave{c})+1\big)\,\grave{s}^3 + \mathcal{R}(\grave{c})\,\big(2\,\dot{\beta}(\grave{c})-1\big)^2\,\grave{s}^2 \\ &\quad - 2\,\mathcal{R}(\grave{c})\,\beta(\grave{c})\,\big(2\,\dot{\beta}(\grave{c})-1\big)\grave{s} + \mathcal{R}(\grave{c})\,\dot{\beta}^2(\grave{c}). \end{aligned} \tag{19c}$$

Notice that Eq. (19b) vanishes on the coincidence curve, see Eq. (6), and Eq. (19c) vanishes at the singular extension locus, see Eq. (16). Those observations together with the hypothesis on β, $\mathcal{R}$ and $\mathcal{D}(s, c)$ implies that for any $(\grave{s}, \grave{c})$ not on the coincidence curve nor on the singular extension locus, all factors of the resultant will be non-null and, therefore, $\mathcal{E}$ and $\mathcal{T}$ will not have any coinciding roots. This proves that at the extension ($\mathcal{E} = 0$) we have transversality ($\mathcal{T} \neq 0$). □

Of course, by setting $\beta \equiv 0$ this transversality disappears.

3 Riemann solution

A typical Riemann solution can be decomposed into a sequence of *constant states* and *wave groups*: groups of elementary waves (shocks or rarefactions) that move together as a single entity. We introduce the notation $P1 \xrightarrow{w} P2$ to express the fact that the states $P1$, $P2$ are connected by an elementary wave w. Here, elementary shocks and rarefactions are saturation or compositional transport waves; they may be slow or fast depending on the ordering between the characteristic speeds, which varies. Deciding if a wave is a s-wave or an c-wave for rarefactions is a matter of verifying which is the associated eigenvalue; for shocks one must verify in which branch of the Hugoniot-locus lies the pair of left, right states.

To construct the Riemann solutions we will use the R-Regions method, for every left-state $\mathbf{L}$, state space will be decomposed into a collection of $N < \infty$

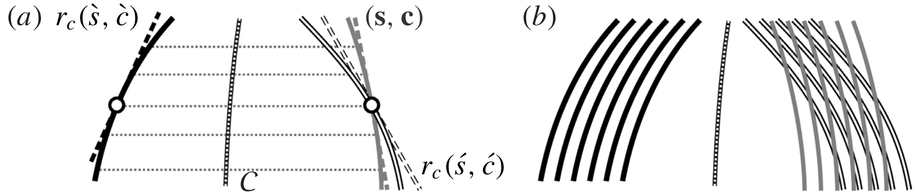

Figure 4: Transversality between the extension of slow compositional rarefaction curves and the corresponding fast compositional rarefaction curves. Figures (a) and (b): solid black lines, slow compositional rarefactions; double lines, fast compositional rarefactions; gray lines, extension of slow compositional rarefactions; railway, coincidence locus. Figure (a): Dashed black line, space spanned by $r_c(\grave{s}, \grave{c})$; Double dashed line, space spanned by $r_c(\acute{s}, \acute{c})$; Dashed gray line, space spanned by $D\mathcal{F}(\grave{s}, \grave{c})r_c(\grave{s}, \grave{c})$; Pointed gray lines, representation of the doubly characteristic shocks between states on the slow compositional rarefaction and its extension (composite curve).

open sets (the R-Regions) which we will denote as K, $1 \leq K \leq N$, such that the Riemann solutions from the fixed left-state $\mathbf{L}$ to the varying right-state $\mathbf{R} \in K$ will possess the same topology. Here, we will use roman numbers to identify the R-Regions, which are depicted in Figure 5.a.

The elementary waves will be written as R for rarefactions and S for shocks. Rarefaction waves may be slow (R^-) or fast (R^+). Shock waves may be slow, fast or doubly characteristic (S^d). The waves may pertain to the compositional family c, or to the saturation family s. We indicate that two adjacent elementary waves join characteristically at an state M by appending a hat: $\widehat{M}$.

The Riemann solutions for any left state $\mathbf{L}$ on the right-hand side of the coincidence and sufficiently close to it are as follows (see Fig. 5.b):

(A) $\mathbf{R}$ states in I, III, $VIII$ and IX. Those regions give rise to classical Lax constructions, the solutions will be briefly described. Here, the intermediate constant state will be denoted by A, B or C, accordingly to the solution.

$$I: \quad \mathbf{L} \xrightarrow{S_s^-} A \xrightarrow{S_c^+} \mathbf{R}, \qquad III: \quad \mathbf{L} \xrightarrow{R_s^-} C \xrightarrow{S_c^+} \mathbf{R}, \tag{20a}$$

$$VIII: \quad \mathbf{L} \xrightarrow{R_s^-} C \xrightarrow{R_c^+} \mathbf{R}, \qquad IX: \quad \mathbf{L} \xrightarrow{S_s^-} B \xrightarrow{R_c^+} \mathbf{R}; \tag{20b}$$

(B) $\mathbf{R}$ states in II and IV. In the transition from region I to region II as well as from III to region IV, the fast compositional shock S_c^+ becomes characteristic with respect to the saturation family. The composite wave that follows joins the fast S_c^+ shock with the fast R_s^+ rarefaction at state $\widehat{N}$ (notice that we depict

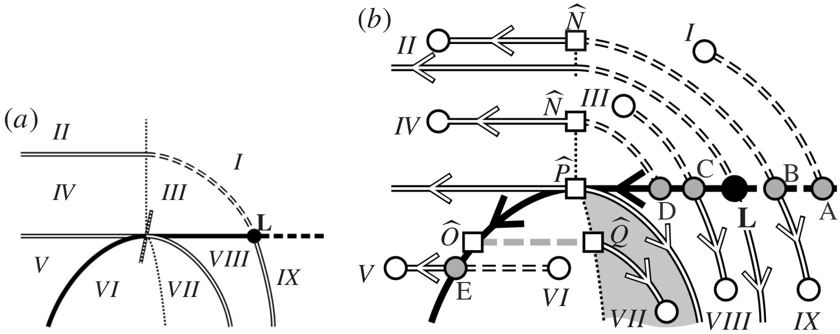

Figure 5: Black circle: **L** left state. Single solid curves with arrows: slow rarefactions. Single dashed curves: slow shocks. Double solid curves with arrows: fast rarefactions. Double dashed curves: fast shocks. Dotted lines: extensions of slow wave curves from **L**. (*a*) Rough draft of the R-Regions. Railway: part of the coincidence curve. (*b*) Stable solutions for $\mathbf{R} \in K$. Gray circles: M states (see relation with letters A to E in section 3). Squares: $\widehat{N}$, $\widehat{O}$, $\widehat{P}$ and $\widehat{Q}$ states. White circles: **R** states. Dashed gray line: doubly characteristic overcompressive shock. Shadowed region: single wave group solution.

the fact that two waves are characteristic by appending a hat on the state that bounds them in the solution). The intermediate constant state B lies on the slow saturation shock curve emanting from **L**, whereas the intermediate constant state D lies on the slow saturation rarefaction curve emanating from **L**. The solution is given as:

$$II: \quad \mathbf{L} \xrightarrow{R_s^-} B \xrightarrow{S_c^+} \widehat{N} \xrightarrow{R_s^+} \mathbf{R}, \qquad IV: \quad \mathbf{L} \xrightarrow{S_s^-} D \xrightarrow{S_c^+} \widehat{N} \xrightarrow{R_s^+} \mathbf{R}. \tag{21}$$

(C) **R** states in V. In the transition from region IV to region V the fast, characteristic, compositional shock S_c^+ ceases to exist. The slow saturation rarefaction R_s^- is followed by a slow compositional rarefaction R_c^- that lies in the left-hand side of the coincidence curve. Those two slow rarefactions join at the state P, which is depicted in the Riemann solution as $\widehat{P}$. The intermediate constant state E lies on the compositional rarefaction curve emanating from state P.

$$V: \quad \mathbf{L} \xrightarrow{R_s^-} \widehat{P} \xrightarrow{R_c^-} E \xrightarrow{R_s^+} \mathbf{R}. \tag{22}$$

(D) **R** states in VI. In the transition from region V to region VI the fast, saturation rarefaction R_s^+ is replaced by a fast, saturation shock S_s^+. This is a classical construction, similar to case $\mathbf{R} \in V$.

$$VI: \quad \mathbf{L} \xrightarrow{R_s^-} \widehat{P} \xrightarrow{R_c^-} E \xrightarrow{S_s^+} \mathbf{R}. \tag{23}$$

(E) **R** states in VII.

This R-Region will contain the Riemann solutions without constant intermediate state. In the transition from region VI to region VII the fast, saturation shock S_s^+ becomes slow, thus it is not an option to reach the **R** states. However, for each O state lying in the rarefaction curve emanating from P, there will correspond a Q state on the extension of the referred rarefaction curve, for which a doubly contact saturation shock can be constructed. From such Q state, an admissible, fast, compositional rarefaction R_c^+ emanate; allowing us to complete the Riemann solution:

$$VII: \quad \mathbf{L} \xrightarrow{R_s^-} \widehat{P} \xrightarrow{R_c^-} \widehat{O} \xrightarrow{S_s^d} \widehat{Q} \xrightarrow{R_c^+} \mathbf{R}. \tag{24}$$

The wave S_s^d is a doubly characteristic compositional shock. This Riemann solution is shown in Figure 6.

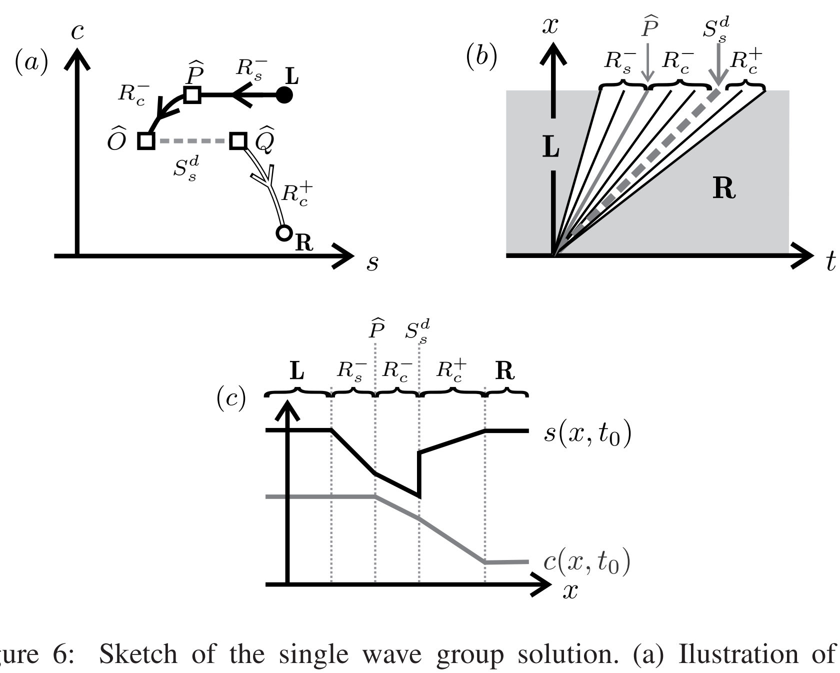

Figure 6: Sketch of the single wave group solution. (a) Ilustration of the wave-curves in state space. (b) Diagram of characteristics in xt plane. (c) Saturation s and composition c profiles for a fixed time.

4 Single wave group for arbitrarily small rarefactions

Let a left state **L** be on the left-hand side of the coincidence sufficiently close to it and out of the singular extension locus. There exists an open set of right states **R** for which the solution comprises just a single wave group with arbitrarily small compositional rarefactions waves, see Figure 7. This is a direct consequence of Lemma 3, therefore, it holds for every model in our family.

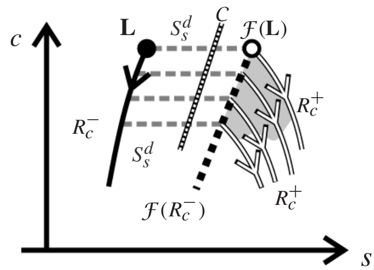

Figure 7: Sketch of the single wave group solution for arbitrarily small compositional rarefactions. Black dot: left state, **L**. White dot: extension of **L**, $\mathcal{F}(\mathbf{L})$. Solid line with arrows: slow compositional rarefaction, R_c^-. Dashed gray line: doubly characteristic shocks, S_s^d. Railway: coincidence locus. Dotted line: extension of the slow compositional rarefaction, $\mathcal{F}(R_c^-)$. Double line with arrows: fast compositional rarefactions, R_c^+. Shadowed area: R-region where the single wave group solution for arbitrarily small compositional rarefactions holds.

We performed numerical experiments using the standard PDE integration method and verified that, for our choices of the functions $\mathcal{R}$ and β, the Riemann solutions without intermediate constant state persisted under perturbations of the left and right states. See an example of a Riemann problem simulated in Figure 8.

References

[1] F. Furtado. *Structural stability of nonlinear waves for conservation laws*. Ph.D. thesis, NYU (1989).

[2] E. Isaacson, D. Marchesin and B. Plohr. *Transitional waves for conservation laws*. SIAM J. Math. Anal., **21**(4) (1990), 837–866.

[3] E.L. Isaacson and J.B. Temple. *Analysis of a singular hyperbolic system of conservation laws*. Journal of Differential Equations, **65**(2) (1986), 250–268.

[4] T. Johansen and R. Winther. *The solution of the Riemann problem for a hyperbolic system of conservation laws modeling polymer flooding*. SIAM J. Math. Anal., **19**(3) (1988), 541–566.

[5] B. Keyfitz and H. Kranzer. *A system of non-strictly hyperbolic conservation laws arising in elasticity theory*. Arch. Rational Mech. Anal., **72** (1980), 219–241.

[6] P. Lax. *Hyperbolic systems of conservation laws II*. Comm. Pure Appl. Math., **10** (1957), 537–566.

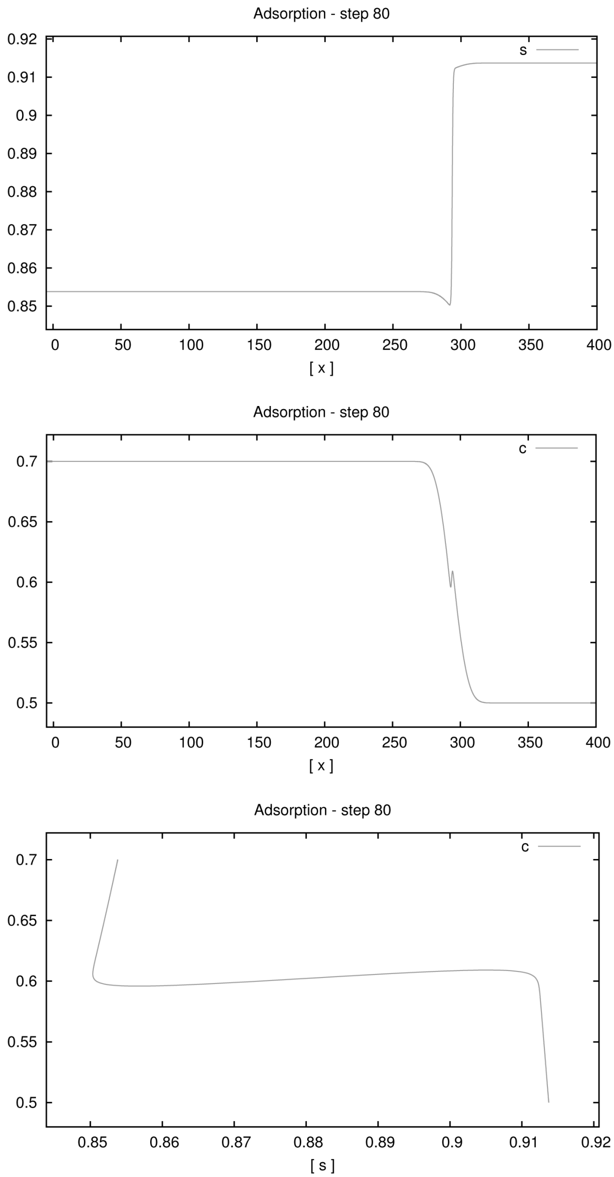

Figure 8: Numerical simulation of the single wave group solution. Parameters and data: $\beta(c) = 0.3\,c + 0.1\,c^2$, $\mathcal{R}(c) = 2.0 + 0.6\,c - 0.2\,c^2$, $\mathbf{L} = (0.8538\,,\,0.7000)$ and $\mathbf{R} = (0.9137\,,\,0.5000)$.

[7] T.-P. Liu. *The Riemann problem for general* 2×2 *conservation laws*. Trans. AMS, **199** (1974), 89–112.

[8] T.P. Liu and C.H. Wang. *On a nonstrictly hyperbolic system of conservation laws*. J. Differential Equations, **57**(1) (1985), 1–14.

[9] Maplesoft. *Maple 13*, 2009, Maplesoft, a division of Waterloo Maple Inc, Waterloo, Ontario, Canada.

[10] V. Matos and D. Marchesin. *Large viscous solutions for small data in systems of conservation laws that change type*. J. Hyperb. Diff. Eq., **2** (2008), 257–278.

[11] J.D. Silva. *Organizing structures in the Riemann solution for thermal multiphase flow in porous media*. Ph.D. thesis, IMPA, Brazil (2011).

[12] J.D. Silva and D. Marchesin. *Riemann solutions without an intermediate constant state for a system of two conservation laws*. Journal of Differential Equations, **256**(4) (2014), 1295–1316.

[13] S. Schecter, D. Marchesin and B.J. Plohr. *Structurally stable Riemann solutions*. Journal of Differential Equations, **126**(2) (1996), 303–354.

Vitor Matos
Centro de Matemática
Faculdade de Economia
Universidade do Porto
Rua Dr. Roberto Frias, 4200-464
Porto
PORTUGAL

E-mail: vmatos@fep.up.pt

Julio D. Silva
University of Calgary
Department of Computer Science
ICT 602, 2500 University Dr NW
Calgary, Alberta
T2N 1N4
CANADA

E-mail: jd.silva@ucalgary.ca

Dan Marchesin
Instituto Nacional de Matemática Pura e Aplicada (IMPA)
Estrada Dona Castorina, 110
22460-320 Rio de Janeiro, RJ
BRAZIL

E-mail: marchesi@fluid.impa.br